IRSTI 29.17.11 https://doi.org/10.26577/RCPh20259436

M. Kavehnia[1], H. Sadeghi[1*], S.N. Hosseinimotlagh[2]
[1]Department of Physics, Faculty of Sciences, Arak University, Arak, Iran
[2]Department of Physics, Shi.,C., Islamic Azad University, Shiraz, Iran
*e-mail: H-sadeghi@araku.ac.ir

UTILIZING THE EFFECTIVE INTERACTION POTENTIALS TO INVESTIGATE THE HOT THERMAL RELAXATION INDUCED VIA ION AND ELECTRON TEMPERATURE OF DT, D^3He AND $P^{11}B$ HOT PLASMA

In this work, the binary model and the effective interaction potentials approach are used to investigate the hot thermal relaxation induced by the temperature of dense plasma. This model is significant for thermonuclear combustion, especially for non-isothermal dense hot plasma fuels such as DT (neutron generator). Therefore, we used the development of this model for the first time to physically describe two neutron-free fuels D^3He and $P^{11}B$. In this study, we examine the temperatures of electrons (Te) and ions (Ti) individually because the temperature within the electron and ion subsystems attains equilibrium much more rapidly than the temperature between electrons and ions. This phenomenon arises from the disparity between the masses of ions and electrons. Since the simulations and computations for fusion through confinement are exceedingly intricate due to the multitude of different physical processes that occur, and a considerable amount of time is required to perform these calculations, we have applied the method of effective interaction potentials for the first time in this study as this method can facilitate precise and rapid calculations for dense plasmas. The effective interaction potentials consist of two components: a) charge overlap effects at extended distances and b) quantum effects at shorter distances. We compute the stopping power, deceleration time, transfer coefficients, energy absorption, and temperature relaxation associated with non-isothermal dense hot plasma of DT, D^3He, and $P^{11}B$ fuels, identifying their optimal values.

Keywords: dense, fusion fuel, hot plasma, temperature, interaction potential.

М. Кавехния[1], Х. Садеги[1*], С.Н. Хоссейнимолаг[2]
[1]Физика кафедрасы, Ғылым факультеті, Арак университеті, Арак, Иран
[2]Физика кафедрасы, Шираз, Ислам Азад университеті, Шираз, Иран
*e-mail: H-sadeghi@araku.ac.ir

DT, D^3He және $P^{11}B$ ыстық плазмасының иондық және электрондық температурасы арқылы индукцияланған ыстық термиялық релаксацияны зерттеу үшін тиімді өзара әрекеттесу потенциалдарын пайдалану

Бұл жұмыста тығыз плазма температурасымен индукцияланған ыстық термиялық релаксацияны зерттеу үшін екілік модель және тиімді өзара әрекеттесу потенциалдары тәсілі қолданылады. Бұл модель термоядролық жану үшін, әсіресе DT (нейтрон генераторы) сияқты изотермиялық емес тығыз ыстық плазма отындары үшін маңызды. Сондықтан біз бұл модельдің дамуын алғаш рет екі нейтронсыз отын D^3He және $P^{11}B$ физикалық түрде сипаттау үшін пайдаландық. Бұл зерттеуде біз электрондардың (Te) және иондардың (Ti) температурасын жеке-жеке қарастырамыз, себебі электрон мен иондық жүйелердегі температура электрондар мен иондар арасындағы температураға қарағанда әлдеқайда жылдам тепе-теңдікке жетеді. Бұл құбылыс иондар мен электрондардың массалары арасындағы айырмашылықтан туындайды. Шектелген термоядролық синтезді модельдеу және есептеулер көптеген әртүрлі физикалық процестерге байланысты өте күрделі болғандықтан және бұл есептеулерді орындау үшін айтарлықтай уақыт қажет болғандықтан, біз бұл зерттеуде алғаш рет тиімді өзара әрекеттесу потенциалдары әдісін

қолдандық, себебі бұл әдіс тығыз плазмалар үшін дәл және жылдам есептеулерді жеңілдете алады. Тиімді өзара әрекеттесу потенциалдары екі компоненттен тұрады: а) ұзақ қашықтықтағы зарядтардың қабаттасу эффектілері және ә) қысқа қашықтықтағы кванттық эффектілер. Біз DT, D^3He және $P^{11}B$ отындарының изотермиялық емес тығыз ыстық плазмасымен байланысты тоқтату қуатын, баяулау уақытын, тасымалдау коэффициенттерін, энергияны сіңіруді және температураның релаксациясын есептейміз, олардың оңтайлы мәндерін анықтаймыз.

Түйін сөздер: тығыздық, термоядролық отын, ыстық плазма, температура, өзара әрекеттесу потенциалы.

М. Кавехния[1], Х. Садеги[1]*, С.Н. Хоссейнимолаг[2]
[1]Кафедра физики, факультет естественных наук, Университет Арака, Арак, Иран
[2]Кафедра физики, Исламский университет Азад, Шираз, Иран
*e-mail: H-sadeghi@araku.ac.ir

Использование эффективных потенциалов взаимодействия для исследования горячей тепловой релаксации, индуцированной ионной и электронной температурой горячей плазмы DT, D^3He и $P^{11}B$

В данной работе бинарная модель и подход эффективных потенциалов взаимодействия используются для исследования горячей тепловой релаксации, индуцированной температурой плотной плазмы. Эта модель важна для термоядерного горения, особенно для неизотермических плотных плазменно-горячих топлив, таких как DT (нейтронный генератор). Поэтому мы впервые использовали разработку этой модели для физического описания двух безнейтронных топлив D^3He и $P^{11}B$. В данном исследовании мы рассматриваем температуры электронов (Te) и ионов (Ti) по отдельности, поскольку температура внутри электронной и ионной подсистем достигает равновесия гораздо быстрее, чем температура между электронами и ионами. Это явление возникает из-за разницы в массах ионов и электронов. Поскольку моделирование и расчёты для термоядерного синтеза в условиях удержания чрезвычайно сложны из-за множества различных физических процессов, которые происходят, и для выполнения этих расчётов требуется значительное время, мы впервые применили в данном исследовании метод эффективных потенциалов взаимодействия, поскольку этот метод может обеспечить точные и быстрые расчёты для плотной плазмы. Эффективные потенциалы взаимодействия состоят из двух компонентов: а) эффектов перекрытия зарядов на больших расстояниях и б) квантовых эффектов на более коротких расстояниях. Мы вычисляем тормозную способность, время замедления, коэффициенты переноса, поглощение энергии и температурную релаксацию, связанные с неизотермической плотной горячей плазмой топлив DT, D^3He и $P^{11}B$, и определяем их оптимальные значения.

Ключевые слова: плотность, термоядерное топливо, горячая плазма, температура, потенциал взаимодействия.

Introduction

In a high-temperature hydrogen plasma via inertial confinement fusion (ICF) or in the center of stars, ions undergo fusion reactions to produce energetic alpha particles. Then, the alpha particles give their energy to the ions and electrons that make up the plasma through the Coulomb collision, but their speeds are different because the electrons are lighter than the ions. This causes an imbalance in the temperature of the electron and ion, which causes energy exchange between them to reach the equilibrium temperature. Therefore, the temperature relaxation of electrons and ions is a key parameter that must be modeled to accurately describe the ignition temperature of a thermonuclear plasma [1-4].

Knowledge of the fusion fuel hotspot temperature is critical to the success of inertial confinement fusion (ICF) experiments [3]. In thermonuclear conditions, the fuel is in the form of

plasma, and the ion (Ti) and electron (Te) temperatures should generally be distinguished. The ion temperature can be deduced from the spectrum of the fusion reaction products [5-7]. Information about the electron temperature is mainly obtained from the radiation of the hot blasted plasma, as this radiation is produced by the free electrons scattered off the ions. Since the electrons are much faster, it is only their distribution that dominates the emission spectrum, which should then provide the basis for inferring Te [8-9].

Strongly produced plasmas in experiments are often far from thermal equilibrium. For example, ultra-cold neutral plasmas and dense plasmas can have electron and ion temperatures that differ by an order of magnitude or more [1-5]. In non-equilibrium plasmas - especially those far from equilibrium - an extension of the ideal gas kinetic theory is used to understand the behavior of the plasma [10-12].

In this paper relaxation of temperature, an additional portion of the state equation and correlation energy of non-isothermal hot dense plasmas are investigated according to the effective interaction potentials method, followed by the electron-ion effective interaction potentials for a hot-dense plasma [13-15]. Dense plasma is an active experimental subject and theoretical research is carried out because of its importance for ICF. To obtain a heat-nuclear reaction, study of the transfer properties and relaxation of time caused by the dense plasma temperature is required [15]. During a compression of a target, by a high-energy particle stream, a non-isothermal plasma with different electron and ion temperatures, created. [16-19] Therefore, studying the relaxation of time of the electrons and ions is very important. The temperature inside the electron and ion subsystems reaches equilibrium between electrons and ions much faster [20-21].

This is due to the large difference between the masses of ions and electrons [22-24]. In this method, the effective interaction potential, Φ, which involves collective screening and quantum effects, is given by equation (1):

$$\Phi_{\alpha\beta}(r) = \int \frac{d^3k}{2\pi^2} \frac{\Phi_{\alpha\beta}(r)}{\varepsilon(k,\omega)} e^{ik\cdot r}. \qquad (1)$$

Where $\Phi_{\alpha\beta}(r)$ is the pair interaction potential and $\epsilon(k, \omega)$ is the dielectric function. The simplest model that describes the screening potential of point charges, is the Yukawa potential, which is given by equation (2)

$$\Phi_Y(r; n. T) = \frac{Q_1 Q_2}{r} e^{-k_Y r}. \qquad (2)$$

Where k_Y denotes the determinate inverse Yukawa screening length. The Yukawa potential can be understood by using the Fermi model or the long wavelength range of the polarization function, in the random phase approximation [25]. In this paper, the results of stopping power, transition coefficients and temperature relaxation are investigated using the effective interaction potentials between electrons and ions in dense plasmas. The effective potential is deduced by using a long wavelength extension of the polarization function and quantum potentials, which implies a limited amount of potential interaction at a distant distance.

Effective interaction potential of electron-ion

The dielectric function in the random phase approximation is given by equation (3):

$$\epsilon(k,0) = 1 - \frac{4\pi e^2}{k^2}\Pi_{RPA}(k) - \frac{4\pi Z^2 e^2}{k^2}\Pi_{ion}(k). \qquad (3)$$

Where $\Pi_{ion}(k)$ is the polarization function of the ions and is obtained from the relation: $\Pi_{ion}(k) = -n_i/(k_B T_i)$. Figure 1-a shows that the variations of $\Pi_{ion}(k)$ (ion polarization function) as a function of T_i(keV) for the three fusion reactions DT, D^3He, and $P^{11}B$.

$\Pi_{RPA}(k)$ is the quantum polarization function of electrons at a finite temperature, which is given by equation (4) [26]:

$$\Pi_{RPA}(k.\omega) = -\frac{k^2\chi_0^2}{16\pi e^2 Z^3}[g_3(u+\mathcal{Z}) - g_3(u-\mathcal{Z})]. \qquad (4)$$

Where: $u = \frac{\omega}{kv_F}$, $\mathcal{Z} = \frac{k}{2k_F}$, $\chi_0^2 = 3/16(\hbar\omega_P/E_F)^2$, $k_F = (3\pi^2 n_e)^{1/3}$, $\omega_P^2 = 4\pi n_e e^2/m_e$ and v_F is the Fermi velocity. Figures 1-b and 1-c show that the variations of u and Z as a function of T (keV) and T_i(keV)for three fusion reactions DT, D^3He, and $P^{11}B$, respectively.

Also $g_3(x)$is obtained from equation (5):

$$g_3(x) = -g_3(-x) = \int \frac{ydy}{\exp(y^2/\theta - \eta) + 1} \ln\left|\frac{x+y}{x-y}\right|. \qquad (5)$$

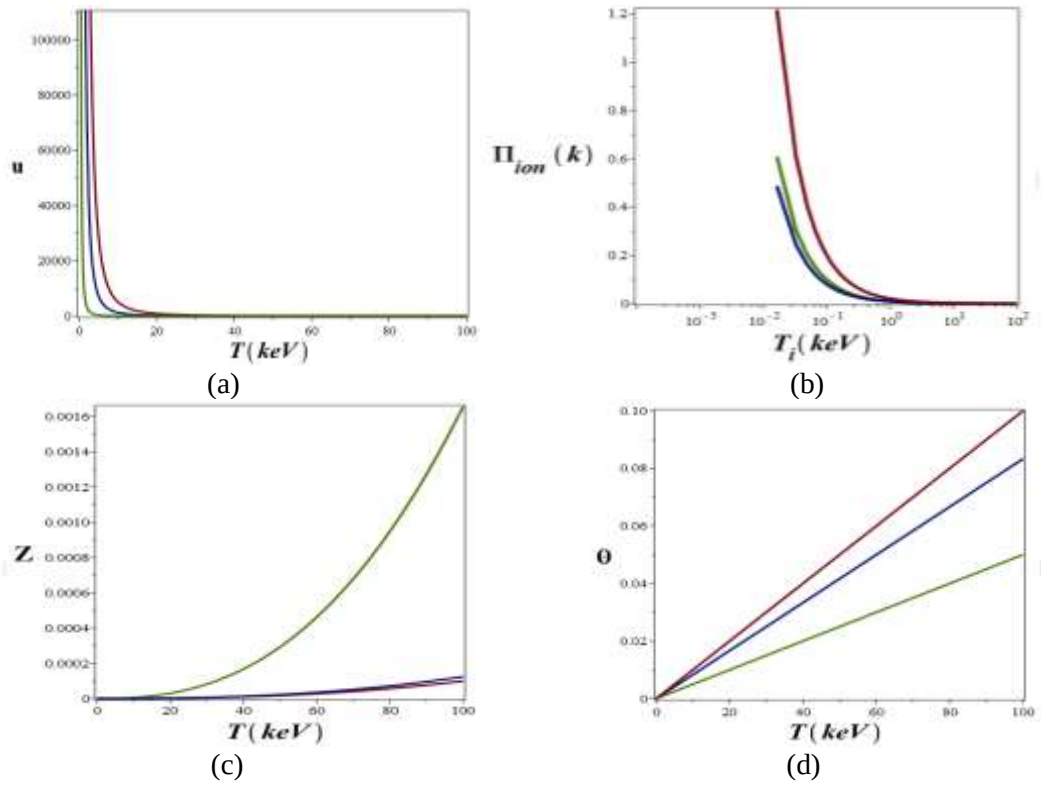

Figure 1 – Comparison of (a): $\mathbf{\Pi_{ion}(k)}$ (ion polarization function). (b) u, (c) Z, and (d) **θ** variations as a function of $\mathbf{T_i(keV)}$ and $\boldsymbol{T}\mathbf{(keV)}$ for three fusion reactions DT(red), D^3He(blue), and $P^{11}B$ (green)

Where θ is the degeneracy parameter, $\theta = k_B T/E_F$ and η is the chemical potential, defined as $\eta = \mu/k_B T$. In Figure 1-d, we observe the variations of θ (the eigenvalue parameter) in terms of T (keV) for three fusion reactions DT, D^3He, and $P^{11}B$. The effective interaction potential of an electron-ion is given by equation (6) [27]:

$$\Phi_{ei} = \frac{Ze^2}{r}[1 - \exp(-r/\lambda_{ei})]. \qquad (6)$$

Where $\lambda_{ei} = \hbar/\sqrt{\pi m_{ei} k_B T_{ei}}$ is the thermal wavelength that describes the nature of the electron wave in the the pair interaction potential, m_{ei} is the reduced mass of the pair particle, and Z is the number of ion charges. Figure 2 shows that the **c**omparison of **t**he three-dimensional diagram of variations $\boldsymbol{\lambda_{ei}}$ (thermal wavelength) as T_i(keV) and T_e(keV) for three fusion reactions DT**,** D^3He**,** and $P^{11}B$.

In order to describe the non-isothermal plasma at two temperatures, not only the temperatures of electrons and ions, but also the electron-ion temperature, T_{ei}, are required [28,29]. Therefore, T_{ei} is represented by equation (7) [30]:

$$T_{ei} = \sqrt{T_e T_i}. \qquad (7)$$

The effective interaction potential of electron-ion Φ_{ei} is represented by equation (8):

$$\Phi_{ei} = \frac{Ze^2}{r\lambda_{ee}^2\gamma^2\sqrt{1-(2\,k_D/\lambda_{ee}\gamma^2)^2}}\left[\left(\frac{1-\lambda_{ee}^2B^2}{1-\lambda_{ei}^2B^2}\right)\exp(-rB) - \left(\frac{1-\lambda_{ee}^2A^2}{1-\lambda_{ei}^2A^2}\right)\exp(-rA)\right] + \frac{Ze^2\exp(-r/\lambda_{ei})}{r(1+C_{ei})}. \qquad (8)$$

Where A^2, B^2, C_{ei}, γ^2 and λ_{ee}^2 and k_i^2 obtained from the equations (9) - (14):

$$A^2 = \gamma^2/2\left[1+\sqrt{1-(2\,k_D/\lambda_{ee}\gamma^2)^2}\right], \qquad (9)$$

$$B^2 = \gamma^2/2\left[1-\sqrt{1-(2\,k_D/\lambda_{ee}\gamma^2)^2}\right], \qquad (10)$$

$$C_{ei} = \left(k_D^2\lambda_{ei}^2 - k_i^2\lambda_{ee}^2\right)/\left(\lambda_{ee}^2/\lambda_{ei}^2 - 1\right), \qquad (11)$$

$$\gamma^2 = k_i^2 + 1/\lambda_{ee}^2, \qquad (12)$$

$$\lambda_{ee}^2 = -b_1/4k_F^2, \qquad (13)$$

$$k_i^2 = 4\pi\, n_i {Z_i}^2 e^2/k_B T_i. \qquad (14)$$

In Figures 3-a to 3-c, we see that the comparison of the three-dimensional diagrams of variations A, B, and C_{ei} in terms of T_i(keV) and T_e(keV) for three fusion reactions DT, D^3He, and $P^{11}B$**,** respectively.

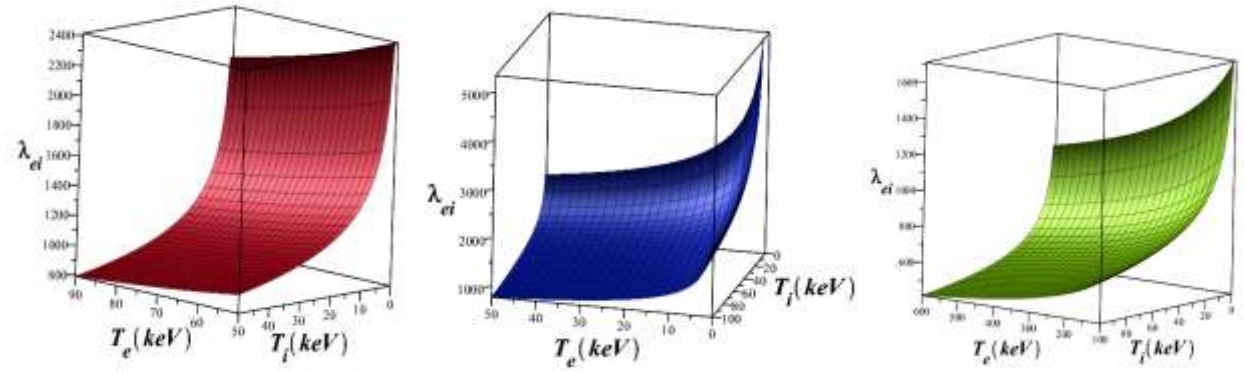

(a) (b) (c)

Figure 2 – Comparison of the three-dimensional diagram of variations $\boldsymbol{\lambda_{ei}}$ (thermal wavelength) as $\mathbf{T_i}$**(keV)** and $\mathbf{T_e}$**(keV)** for three fusion reactions (a) DT (red), (b) D^3He(blue), and (c)$P^{11}B$(green)

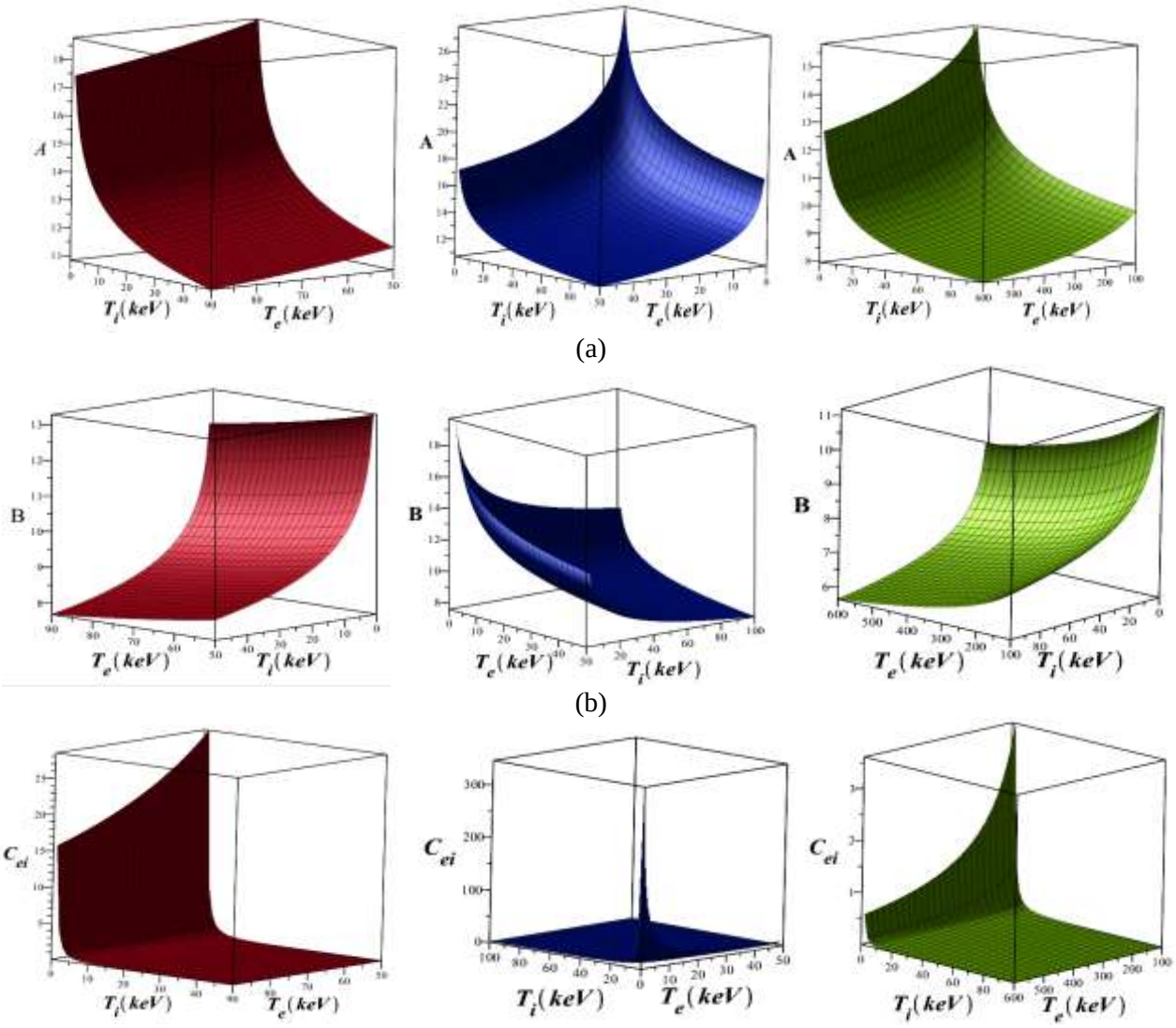

(a)

(b)

(c)

Figure 3 – Comparison of the three-dimensional diagram of variations (a) A, (b)B, and (c) C_{ei} as a function of T_i(keV) and T_e(keV) for three fusion reactions DT (red), D^3He(blue), and $P^{11}B$(green)

Figure 4-a shows that the variations of γ^2) parameter as a function of T_i(keV) for the three fusion reactions DT, D^3He, and $P^{11}B$.

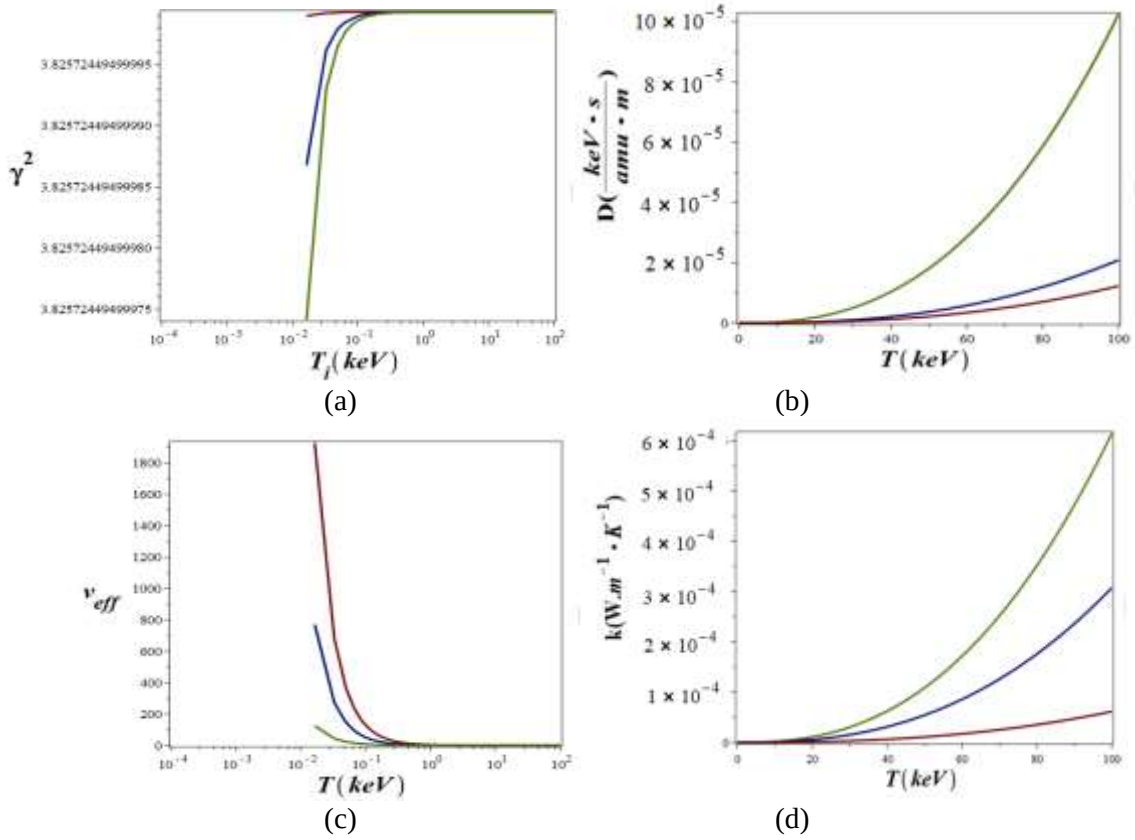

Figure 4 – Comparison of the variations of (a) $\boldsymbol{\gamma^2}$, (b) D (plasma diffusion coefficient), (c) k (thermal conductivity coefficient of plasma) and (d) $\boldsymbol{\nu_{eff}}$ (effective collision frequency) as a function of $\mathbf{T_i}(\mathbf{keV})$ and $\boldsymbol{T}(\mathbf{keV})$for the three fusion reactions DT(red), D^3He(blue), and $P^{11}B$ (green)

Stopping power

One of the most important features that describes the interaction of ions with materials is the stopping power [30]. Stopping power describes the rate of kinetic energy loss of the projectile's direct motion of the projectile in the material, which is presented by the equation (15) [31, 32]:

$$\frac{dE}{dx} = 8\pi n\left(\frac{m_{ei}}{m_i}\right)\cdot E_c \cdot \rho_\perp^2 \cdot \Lambda_{ei}. \qquad (15)$$

Where $E_c = \frac{1}{2}m_{ei}v^2$the center of mass energy of the particles is, m_{ei} is the reduced mass of the ions or electrons. V is relative velocity of the scattered particles and: $\rho_\perp = Ze^2/2E_c$ Also, Λ_{ei} is Coulomb logarithm of the electron-ion that is determined by the scattering angle in equation (16) [33]:

$$\Lambda_{ei} = \frac{1}{\rho_\perp^2}\int_0^\infty \sin^2\left[\frac{\chi(\rho)}{2}\right]\rho d\rho. \qquad (16)$$

Transfer properties

It is important to study the transfer properties for ICF and solid-state physics. In particular, the ICF requires reliable information on the transfer coefficients, that is, the plasma diffusion coefficient D, the thermal conductivity coefficient k, which is obtained from equations (17) and (18) respectively.

$$D = \frac{k_B T}{m_e \nu_{eff}}. \qquad (17)$$

$$k = \frac{5 n_e {k_B}^2 T}{m_e \nu_{eff}}. \qquad (18)$$

Figures 4-b and 4-c show that the variations of D (plasma diffusion coefficient) and k as a function of T (keV) for the three fusion reactions DT, D^3He, and $P^{11}B$, respectively.

In this paper, the DT and D^3He, and $P^{11}B$ dense plasmas are considered. The plasma diffusion

coefficient and the plasma thermal conductivity coefficient with the effective collision frequency are related by equation (19):

$$\nu_{eff} = (4/3)\sqrt{2\pi}e^4\Lambda_{ei}/\sqrt{m_e}(k_BT)^{3/2}. \quad (19)$$

Figure 4-d, shows that the variations of ν_{eff} (effective collision frequency) in terms of T(keV) for three fusion reactions DT, D^3He, and $P^{11}B$, respectively.

Temperature relaxation

The temperature relaxation in plasma is calculated for different density values based on the Coulomb logarithm and using effective potentials [33-34]. The electron-ion temperature relaxation rate (rate of energy change) is determined by as the variations in the mean electron and ion temperatures by the equation (20):

$$\frac{dT_e}{dt} = \frac{T_i - T_e}{\tau_{ei}} . \frac{dT_i}{dt} = \frac{T_e - T_i}{\tau_{ei}}. \quad (20)$$

Where $\tau_{ei}$the electron-ion interaction is time, which can be determined from equation (20) and is equation (21):

$$\tau_{ei} = \frac{3m_em_i}{8\sqrt{2\pi ne^2}\Lambda_{ei}}\left(\frac{k_BT_e}{m_e} + \frac{k_BT_i}{m_i}\right)^{3/2}. \quad (21)$$

Figure 5 illustrates that the comparison of three-dimensional variations of τ_{ei} (ion and electron interaction time) in terms of T_i(keV) and T_e(keV) for the three fusion reactions DT, D^3He, and $P^{11}B$, respectively.

The equation of state for plasma is presented by equation (22):

$$P = P_{ideal} + \frac{2\pi}{3}\sum_{\alpha.\beta}\frac{n_\alpha n_\beta e_\alpha^2 e_\beta^2}{k_BT_{\alpha\beta}\gamma^2\sqrt{1-(2k_D/\lambda_{ee}\gamma^2)^2}} \times \left[\frac{1/{\lambda_{ee}}^2 - B^2}{B\left(1-B^2{\lambda_{\alpha\beta}}^2\right)} - \frac{1/{\lambda_{ee}}^2 - A^2}{A\left(1+A^2{\lambda_{\alpha\beta}}^2\right)}\right] + P_\lambda. \quad (22)$$

In which P_{ideal} is the ideal gas pressure of the plasma. Figures 6 and 7 show that the variations of P_{ideal} (ideal gas pressure) as a function of T and P (plasma pressure) in terms of T_i(keV) and T_e(keV) for three fusion reactions DT, D^3He, and $P^{11}B$, respectively.

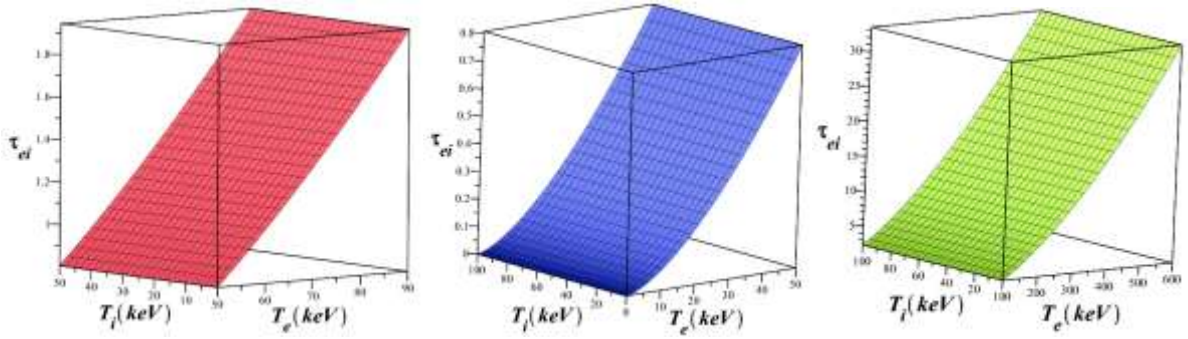

(a) (b) (c)

Figure 5 – Comparison of the three-dimensional diagram of variationsτ_{ei} as a function of T_i(keV) and T_e(keV) for three fusion reactions (a) DT (red), (b)D^3He(blue), and (c) $P^{11}B$(green)

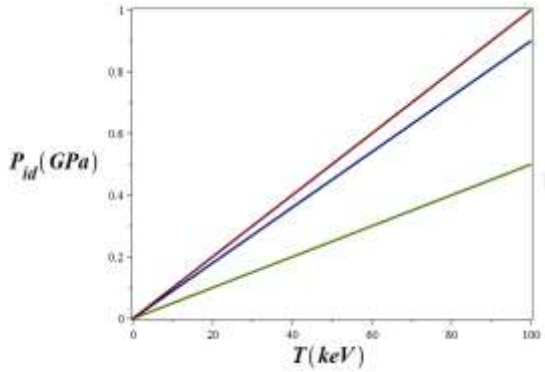

Figure 6 – Variations of $\mathbf{P_{ideal}}$ (ideal gas pressure) as a function of T (keV) for three fusion reactions: (a) DT, (b) D^3He, and (c) $P^{11}B$

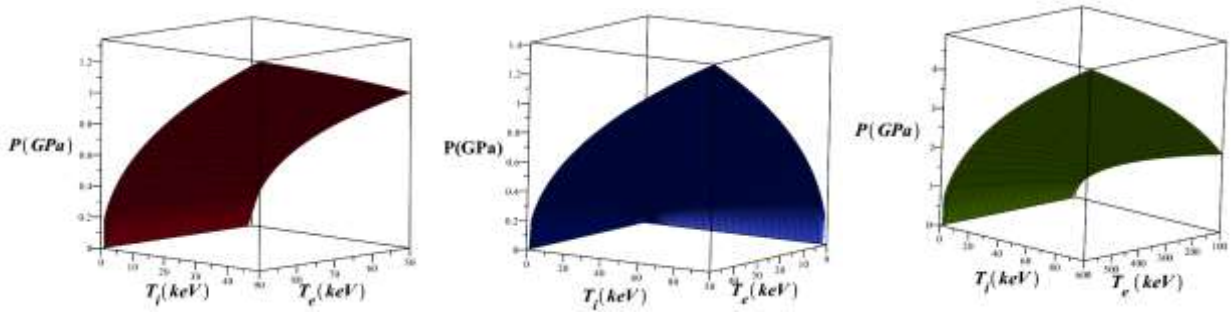

(a) (b) (c)

Figure 7 – Comparisons of the three-dimensional variations of P (plasma pressure) in terms of $\mathbf{T_i(keV)}$ and $\mathbf{T_e(keV)}$ for three fusion reactions (a) DT (red), (b) D^3He (blue), and (c) $P^{11}B$ (green)

P_λ is obtained from equation (23):

$$P_\lambda = 2\pi e^2\{2Z_i n_i n_e \lambda_{ei}{}^2 - n_e{}^2 \lambda_{ee}{}^2 + Z_i n_i n_e \lambda_{ei} e^2/[12 k_B T_{ei}(1 + C_{ei})]\}. \quad (23)$$

For efficient burning, the net energy generated in hot spots should be positive. The energy generated inside the hot spot must compensate for all energy losses. The energy losses inside the hot spot are due to electron-ion collisions, Compton scattering, bremsstrahlung radiation, and radiation. At higher densities required for ignition, the temperature is reduced. Now, if we consider, in addition to the ion temperature T_i(keV) and the electron temperature T_e (keV), the radiation temperature T_r(keV) that is the radiation from the hot spot, we will describe the plasma with a three-temperature model [35-38].

The initial hot spot, has radius r_0 and volume V_0. The initial temperature T_0 and the initial density ρ_0 are defined by other parameters. The total internal energy of ions in a hot spot at time t is given by the equation (24):

$$E_i = \rho_0 V C_{Vi} K_B T_i. \quad (24)$$

In which C_{Vi} is a special ion heat at a fixed value, T_i (keV) is the ion temperature, and V is the volume at time t. Figure 8 shows that the comparison of the three-dimensional variations of E_i (total internal energy of ions in hot spot) as a function of r (cm) and T_i (keV) for three fusion reactions DT, D^3He, and $P^{11}B$, respectively.

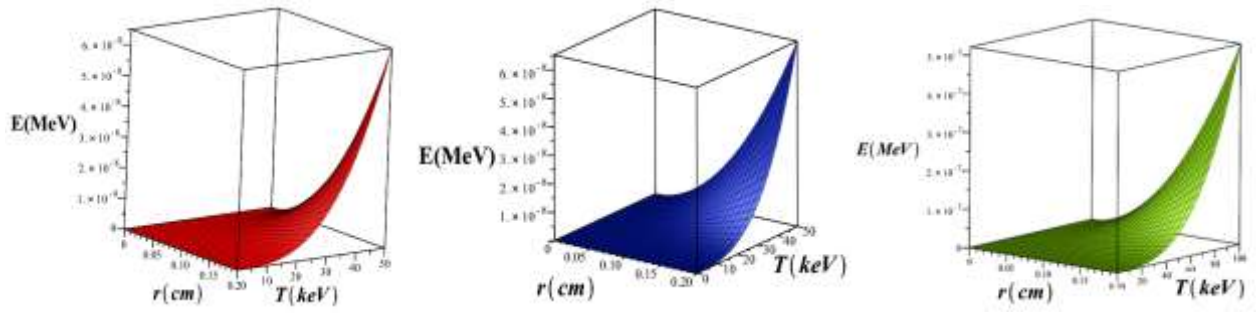

(a) (b) (c)

Figure 8 – Comparison of the three -dimensional diagram of variations E_i (total internal energy of ions in the hotspot) as a function of r and T_i(keV) for three fusion reactions (a) DT (red), (b) D^3He(blue), and (c) $P^{11}B$ (green)

The rate of E_i can be expressed as equation (25):

$$\frac{dE_i}{dt} = V_{\tilde{q}_i}(r.T_i.T_e). \quad (25)$$

Where, $\tilde{q}_i$ is the net energy production rate of ions per unit volume, which depends on the radius of the hot spot, r, at time t, the ion temperature, T_i (keV), and the electron temperature, T_e (keV), and $V = \frac{4}{3}\pi r^3$, where V is the volume of the fuel pellet. The classical values of the specific ion heat in a constant volume:$C_{Vi} = \frac{3}{2}\frac{k_B}{\bar{m}_i}$ and the specific electron heat in a

constant volume: $C_{Ve} = \frac{3}{2}\frac{\bar{Z}k_B}{\bar{m}_i}$. In which k_B is Boltzmann's constant, $\bar{m}_i$ is the mean mass of ions, $\bar{Z}$ is the average atomic number. It is assumed that the plasma is completely ionized. The specific radiation energy is: $E_r = (1/\rho_0)(4\,\sigma_B/c)T_r^4$, in which c is the speed of light and the σ_B is Stefan constant. The specific relation energy in a constant volume is: $C_{Vr} = \frac{1}{\rho_0}\frac{16\sigma_B}{c}T_r^3$. Figures 9-a and 9-b, shows that the variations of E_r (specific relation energy) and C_{Vr} (specific relation heat) as a function of T_r (keV), respectively.

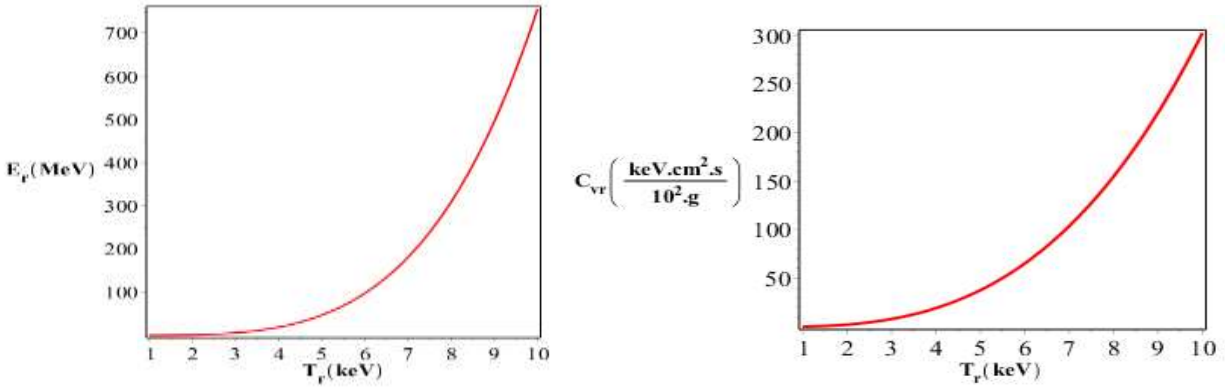

(a) (b)

Figure 9 – Variations of (a) $\mathbf{E_r}$ (special relation energy) and (b) $\mathbf{C_{Vr}}$ (special relation heat) as a function of $\mathbf{T_r(keV)}$

Net Energy Release Rates

The net energy release rates for ions are characterized by the relation (26):

$$q_i(x.\,T_i\,.\,T_e) \equiv S_i - A_{ie}(T_i - T_e). \qquad (26)$$

Where S_i denotes the energy deposition to ions. Because the size of the alpha particle is much smaller than the size of the hot spot, it is assumed that all this energy is deposited in the hot spot. The energy loss of ions due to ion-electron collisions has been investigated, and $A_{ei} = C_{Ve} \times \nu_{eq}$ is the energy transfer coefficient from electron to ion in which ν_{eq} is the frequency of ion collisions with electrons. When $T_i = T_e$, the energy transfer by collisions is zero. The collision frequency is given by equation (27):

$$\nu_{eq} = \frac{8\sqrt{2\pi}}{3}\sqrt{m_e}e^4N_A^2\frac{\bar{Z}^2}{\bar{A}^2}\ln(\Lambda_{ei})\frac{\rho_0}{(k_BT_e)^{3/2}} \times \left(1 - \frac{3}{2}\frac{K_BT_i}{K_BT_e}\frac{m_e}{\bar{m}_i}\right). \qquad (27)$$

Where m_e is the mass of the electron, e is the electron charge, N_A is the Avogadro's number, and $\bar{Z}$ and $\bar{A}$ are the atomic number and atomic weight respectively. Figures 10-a and 10-b, show that the comparisons of the three-dimensional variations of A_{ei} (energy transfer coefficient between electrons and ions) and ν_{eq} (frequency of ion collisions with electrons) as a function of T_i(keV) and T_e(keV) for three fusion reactions DT, D^3He, and $P^{11}B$, respectively.

The Coulomb logarithm $\ln(\Lambda_{ei})$ is obtained by using relation (28):

$$\ln(\Lambda_{ei}) = \max\left[1.\frac{1}{2e^3}\left(\frac{\bar{A}k_B^3}{\bar{Z}\pi N_A\rho_0}\right)^{1/2}T_e^{3/2} \times \left[\bar{Z} + \frac{1}{2\alpha_F}\left(\frac{3k_BT_e}{m_ec^2}\right)^{1/2}\right]^{-1}\right] \qquad (28)$$

where α_F is a structure constant.

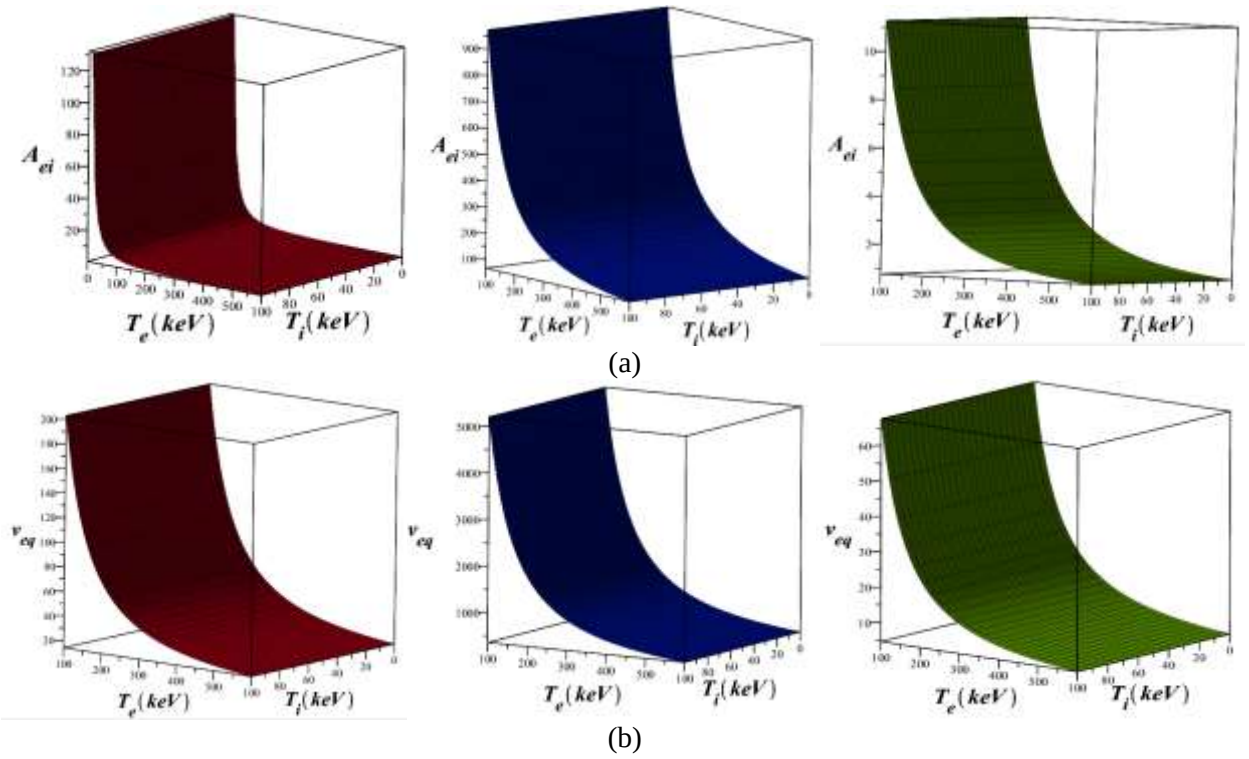

Figure 10 – Comparisons of the three-dimensional variations of (a)Aei (energy transfer coefficient between electron and ion) and (b) ν_{eq} (frequency of ion collisions with electrons) as a function of T_i(keV) and T_e(keV) for three fusion reactions DT (red), D^3He(blue), and $P^{11}B$(green)

Electrons

Apart from the energy given directly to electrons by charged particles, the electron-ion and electron-radiation energy exchanges, q_e, also change the electron temperature. Therefore q_e signifies that the energy release of electrons in a fuel can be expressed as relation (29):

$$q_e(x.T_i\,.T_e.T_r) = S_e + A_{ie}(T_i - T_e) - (A_{er} + A_c)(T_e - T_r). \quad (29)$$

The coefficient A_{er}, which determines the energy transfer coefficient between electrons and radiation, is given by equation (30):

$$A_{er} = 2\left[\frac{2^5}{3}\,\frac{N_{ion}^2\bar{Z}^3e^6\rho_0}{hm_ec^3}\right]\left(\frac{2\pi k_B}{m_eK_BT_e}\right)^{1/2} \quad (30)$$

Where N_{ion} is the total number of ions per cm^3, and S_e is the energy deposition of electrons in the fuel. Figure 11 shows that the variations of A_{er} (the energy transfer coefficient between electron and radiation) as a function of T_e(keV) for three fusion reactions DT, D^3He, and $P^{11}B$, respectively.

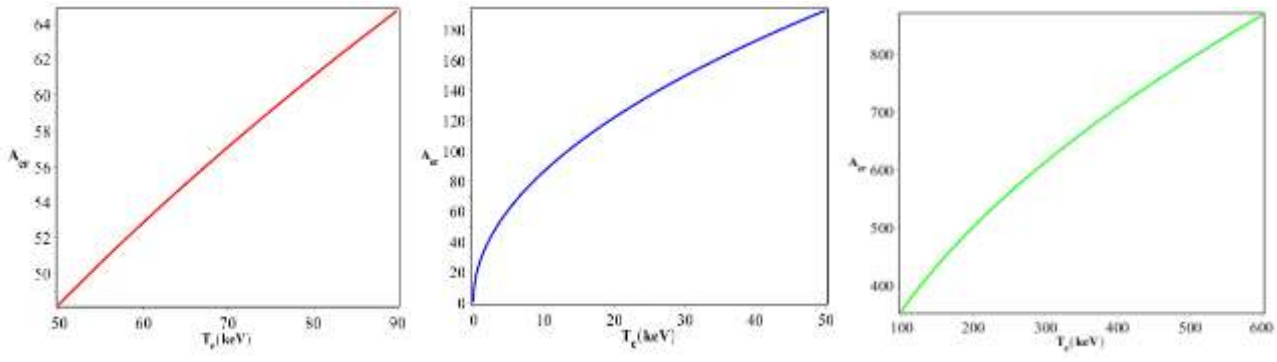

Figure 11 – Variations of $\mathbf{A_{er}}$ (the energy transfer coefficient between electrons and radiation) as a function of $\mathbf{T_e(keV)}$ for three fusion reactions: (a) DT, (b) D^3He, and (c) $P^{11}B$

Apart from radiation, the electron can transmit energy through scattering. The energy transfer coefficient A_c is as equation (31):

$$A_c = \frac{128}{3}\frac{\pi}{m_e c^2}\sigma_B N_e r_c^2 K_B T_r^4. \qquad (31)$$

Where N_e and r_c respectively represent the number of electrons per cm^3 and the classical radius of the electron. σ_B is Stefan's constant [34]. The unit factors A_{ie}, A_{er}, and A_c, is $\frac{MJ}{cm^3 skeV}$. Figure 12 shows that the variations of A_c (energy transfer coefficient) as a function of T_r.

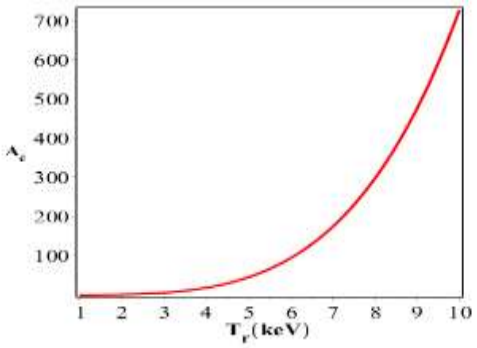

Figure 12 – Variations of $\mathbf{A_c}$ (energy transfer coefficient) as a function of $\mathbf{T_r(keV)}$

Radiation

The net energy gain of the radiation component (q_r) is given by equation (32). Figure 13, shows that the comparisons of three-dimensional variations of q_r (net energy gain of radiation component) as a function of T_r(keV) and T_e(keV) for three fusion reactions DT, D^3He, and $P^{11}B$, respectively.

$$q_r(x.T_e.T_r) = (A_{er} - A_c)(K_B T_e - K_B T_r) - \frac{3\sigma_B K_B T_r^4}{\rho_0 x}. \qquad (32)$$

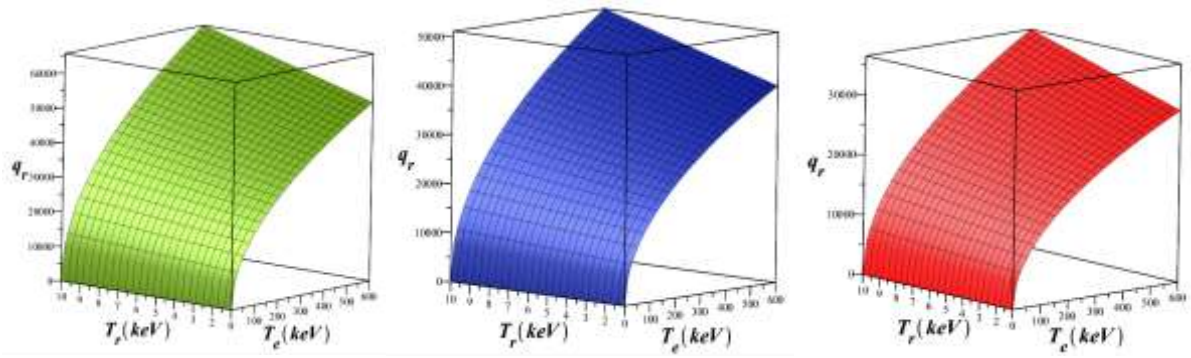

(a) (b) (c)

Figure 13 – Comparisons of the three-dimensional diagram of variations $\mathbf{q_r}$ (net energy gain of the radiation component) as a function of $\mathbf{T_r(keV)}$ and $\mathbf{T_e(keV)}$ for the three fusion reactions (a) DT (red), (b) D^3He(blue), (c) and $P^{11}B$ (green)

Results and discussion

It is clear that from the presented figures, the variations of interaction time of ions and electrons (τ_{ei}) and plasma pressure (P) for the three fusion reactions DT and D^3He and $P^{11}B$ as a function of T_i(keV) and T_e(keV), τ_{ei} is fixed at different ion temperatures and decreases with increasing the electron temperature ,while P decreases at different ion temperatures and increases with increasing electron temperature. The highest value of τ_{ei} is belongs to $P^{11}B$, followed by DT and D^3He, respectively. Meanwhile, the maximum value of P, is belong to $P^{11}B$, D^3He and DT, respectively. Additionally ,our calculations related to variations of $\mathcal{Z}$, plasma degeneracy parameter (θ), plasma effective interaction potential (γ^2), ideal gas pressure (P_{ideal}), plasma diffusion coefficient (D), plasma thermal conductivity coefficient (k) as a function of T (keV), for the three DT and D^3He and $P^{11}B$ fusion reactions,

show that the similar behavior such that with increasing temperature, they remain fixed initially and then increased. The highest values for Z, θ, k, P_{ideal} and D are belong to $P^{11}B$, D^3He, and DT, respectively. While maximum value of γ^2, belongs to DT, followed by D^3He and $P^{11}B$, respectively.

Furthermore, this paper addresses the variations of key plasma parameters in terms of ion temperature T_i(keV) and the electron temperature T_e(keV), such as u, the effective collision frequency (ν_{eff}), $\Pi_{ion}(k)$ (ion polarization function), thermal wavelength (λ_{ei}), A, B and C_{ei} for three fusion reactions of DT , D^3He ,and $P^{11}B$. Our calculations regarding these parameters show that with increasing ion temperature and electron temperatures, they exhibit similar behavior, decreasing initially, then becoming fixed and finally reaching their maximum values. The u value of D^3He> $P^{11}B$ >DT, Also, the numerical values variations of parameters ν_{eff}, A, B, λ_{ei}, and C_{ei} are the similar such that D^3He>DT>$P^{11}B$, but the numerical values for $\Pi_{ion}(k)$ is DT> D^3He >$P^{11}B$ .A summary of the results of our calculations for different key parameters is provided in Table 1.

Table 1. Summary of the results of our calculations for different parameters

Quantity	DT range	D^3He range	$P^{11}B$ range	Results
u	0< u <100000	0< u <25000	0< u <1200	D^3He > $P^{11}B$ > DT
$\mathcal{Z}$	0< $\mathcal{Z}$ <0.00009	0< $\mathcal{Z}$ <0.0004	0< $\mathcal{Z}$ <0.008	$P^{11}B$ > D^3He > DT
θ	0< θ <0.10	0< θ <0.18	0< θ <0.6	$P^{11}B$ > D^3He > DT
$\Pi_{ion}(k)$	0< $\Pi_{ion}(k)$ <1.2	0< $\Pi_{ion}(k)$ <0.6	0< $\Pi_{ion}(k)$ <0.6	DT > D^3He, $P^{11}B$
λ_{ei}	0< λ_{ei} <2200	0< λ_{ei} <5000	0< λ_{ei} <1800	DT > D^3He > $P^{11}B$
A	0< A <17	0< A <28	0< A <16	D^3He > DT > $P^{11}B$
B	0< B <12	0< B <20	0< B <11	D^3He > DT > $P^{11}B$
γ^2	0< γ^2 <3.826	0< γ^2 <3.826	0< γ^2 <3.825	DT, D^3He> $P^{11}B$
C_{ei}	0< C_{ei} <3	0< C_{ei} <700	0< C_{ei} <14	D^3He > DT > $P^{11}B$
D	0< D<0.000012	0< D <0.00005	0< D <0.00100	$P^{11}B$ > D^3He > DT
k	0< k <0.000006	0< k <0.00025	0< k <0.005	$P^{11}B$ > D^3He> DT
ν_{eff}	0< ν_{eff} <1800	0< ν_{eff} <700	0< ν_{eff} <120	D^3He > DT > $P^{11}B$
τ_{ei}	0<τ_{ei} <2.4	0< τ_{ei} <1	0< τ_{ei} <30	$P^{11}B$ > DT > D^3He
P_{ideal}	0< P_{ideal} <1	0< P_{ideal} <1.8	0< P_{ideal} <6	$P^{11}B$ > D^3He> DT
P	<0.999999999950 P	0< P <0.99999999998	0< P <0.99999999999	$P^{11}B$ > D^3He> DT
E_i	0< E_i <0.00007	0< E_i <0.00014	0< E_i <0.00018	D^3He > $P^{11}B$ > DT
E_r	0<E_r <700	0<E_r <700	0<E_r <700	Independent on selected fuel
C_{Vr}	0< C_{Vr} <300	0< C_{Vr} <300	0<C_{Vr} <300	Independent on selected fuel
A_{ei}	0< A_{ei} <0.10	0< A_{ei} <*0.5*	0< A_{ei} <0.18	D^3He > $P^{11}B$ > DT
ν_{eq}	0< ν_{eq} <2.4	0< ν_{eq} <*0.5*	0< ν_{eq} <1	D^3He > DT > $P^{11}B$
A_{er}	0< A_{er} <64	0< A_{er} <180	0< A_{er} <800	$P^{11}B$ > DT > D^3He
A_c	0< A_c <700	0< A_c <700	0< A_c <700	Independent on selected fuel
q_r	0< q_r <30000	0< q_r <35000	0< q_r <60000	$P^{11}B$ > D^3He > DT

Conclusions

It can be seen from our calculations that the total ion internal energy in the hotspot of the fuel pellet of radius r rises with increasing ion, electron and radiation temperatures for all three-fusion reactions DT, D^3He and $P^{11}B$. The specific radiation energy, specific radiation heat and energy transfer coefficient are functions of radiation temperature and increase with rising radiation temperature for these reactions. The energy transfer coefficient between electrons and radiation is a function of the electron temperature, which increases with rising electron temperature for each of selected fusion reactions. The net gain

depends on the radiation temperature and the electron temperature, which enhance with increasing electron and radiation temperatures for all of selected nuclear fusion reactions .The quantities energy change parameter between electrons and ions and frequency of ion collisions with electrons decrease with increasing electron temperature for each of mentioned reactions, while they increase with rising ion temperature.

References

1 S. Brezlnsek, C.P. Dhard, & M. Jakubowski, Plasma–surface interaction in the stellarator W7-X; conclusions drawn from operation with graphite plasma-facing components, Nucl. Fusion. **62**, 016006 (2022). https://doi.org/10.1088/1741-4326/ac3508

2 S. Adlparvar, S. Miraboutalebi, S.M. Sadat Kiai, & L.Rajaee, Overdense plasma heating in Wendelstein 7-X(W7-X), Stellarator. **7**, 1965–1970 (2017). https://doi.org/10.1016/j.rinp.2017.06.015

3 G.A. Wurden, S.C. Hsu, T.P. Intrator, et al., Magneto-Inertial fusion, J. Fusion Energ. **35**, 69–77 (2016). https://doi.org/10.1007/s10894-015-0038-x

4 S. Ryzhkov, & V. Magneto, Inertial fusion and powerful plasma installations (A Review), Appl. Sci. **13**, 6658 (2023). https://doi.org/10.3390/app13116658

5 Y.C.F. Thio, et al., Plasma-Jet-Driven Magneto-Inertial fusion, Fusion Sci. Technol. **75**, 49–52 (2019). https://doi.org/10.1080/15361055.2019.1598736

6 S.V. Ryzhkov, & A.Y.Chirkov, Alternative Fusion Fuels and Systems, (CRC, Abingdon, UK, 2018).

7 O.V. Gotchev, et al., Laser-driven magnetic-flux compression in high-energy-density plasmas, Phys. Rev. Lett. **103**, 215004 (2009). https://doi.org/10.1103/PhysRevLett.103.215004

8 S.V. Ryzhkov, Magneto-Inertial fusion and powerful plasma installations (A Review), Appl. Sci. **13**, 6658 (2023). **https://doi.org/10.3390/app13116658**

9 Y.C.F. Thio, et al., Plasma-Jet-Driven Magneto-Inertial fusion, Fusion Sci. Technol. **75**, 1–18 (2019).

10 S.V. Ryzhkov, A.Y. Chirkov, Alternative Fusion Fuels and Systems, (CRC: Boca Raton, FL, USA; Taylor & Francis Group:Abingdon, UK, 2018).

11 D. Riley, Generation and characterisation of warm dense matter with in-tense lasers, Plasma Physics and Controlled Fusion **60**, 014033 (2017). https://doi.org/10.1088/1361-6587/aa8dd5

12 K. Falk, Experimental methods for warm dense matter research, High Power Laser Science and Engineering **6** e59 (2018). https://doi.org/10.1017./phl.2018.53

13 M. Bonitz, T. Dornheim, Z. A. Moldabekov, S. Zhang, P. Hamann, H. Käh-lert, A. Filinov, K. Ramakrishna, and J. Vorberger, Ab initio simulation of warm dense matter, Physics of Plasmas **27**, 042710 (2020). https://doi.org/10.1063/1.5143225

14 P.-A. Gourdain, The generation of warm dense matter samples using fast magnetic compression, IEEE Transactions on Plasma Science **43**, 2547–2552 (2015). https://doi.org/10.1109/PPC.2015.7296963

15 P. Knapp, K. Beckwith, K. Cochrane, R. C. Clay III, and T. Mattsson, Experimental validation of dense plasma transport models using the z-machine, Tech. Rep. (Sandia National Lab. (SNL-NM), Albuquerque, NM, United States, 2019).

16 D. Sinars, M. Sweeney, C. Alexander, D. Ampleford, T. Ao, J. Apruzese,C. Aragon, D. Armstrong, K. Austin, T. Awe, et al., Review of pulsed power-driven high energy density physics research on z at Sandia, Physics of Plasmas **27**, 070501 (2020). https://doi.org/10.1063/5.0007476

17 R.T. Prenkle, L.G. Silvestri, M.S. Murillo and S.D. Bergeson, Temperature relaxation in strongly-coupled binary ionic mixtures, Nat. Commun. **13**, 15 (2022). https://doi.org/10.1038/s41467-021-27696-5

18 W.J. Garbett and D.A. Chapman, Ignition calculations using a reduced coupled-mode electron- ion energy exchange model, J. Phys.: Conf. Ser. **688** 012019 (2016). https://doi.org/10.1088/1742-6596/688/1/012019

19 G. Faussurier and C. Blancard, Temperature relaxation in dense plasma mixtures, Phys. Rev. E **94** 033210 (2016). https://doi.org/10.1103/PhysRevE.94.033210

20 P.J. Adrian et al, Measurements of ion-electron energy-transfer cross section in high-energy-density plasmas, Phys. Rev. E **106** L053201 (2022). https://doi.org/10.1103/PhysRevE.106.L053201

21 L.X. Benedict, et al, Molecular dynamics studies of electron-ion temperature equilibration in hydrogen plasmas within the coupled-mode regime, Phys. Rev. E **95** 043202 (2017). https://doi.org/10.1103/PhysRevE.95.043202

22 Q. Ma, J. Dai, Kang D., M.S. Murillo, Y. Hou, Z. Zhao and J. Yuan, Extremely low electron-ion temperature relaxation rates in warm dense hydrogen: interplay between quantum electrons and coupled ions, Phys. Rev. Lett. **122** 015001 (2019). https://doi.org/10.1103/PhysRevLett.122.015001

23 P. Svensson, T. Campbell, F. Graziani, Z. Moldabekov, N. Lyu, V.S. Batista, S. Richardson, S.M. Vinko and G. Gregori, Development of a new quantum trajectory molecular dynamics framework, Philos Trans A Math Phys Eng Sci. **381** 20220325 (2022). https://doi.org/10.1098/rsta.2022.0325

24 C.-Z. Gao, C.-B. Zhang, Y. Cai, Y. Wu, Z.-F. Fan, P. Wang and J.-G. Wang, Assessment of the electron-proton energy relaxation rates extracted from molecular dynamics simulations in weakly-coupled hydrogen plasmas, Phys.Rev. E **107** 015203 (2023). https://doi.org/10.1103/PhysRevE.107.015203

25 L.G. Silvestri, R.T. Sprenkle, S.D. Bergeson, M.S. Murillo, Relaxation of strongly coupled binary ionic mixtures in the coupled mode regime, Phys. Plasmas **28**, 062302 (2021). https://doi.org/10.1063/5.0048030

26 S. Rightley, S.D. Baalrud, Kinetic model for electron-ion transport in warm dense matter, Phys. Rev. E **103**, 063206 (2021). https://doi.org/10.1103/PhysRevE.103.063206

27 J. Daligault, On the quantum Landau collision operator and electron collisions in dense plasmas, Phys. Plasmas **23**, 032706 (2016). https://doi.org/10.1063/1.4944392

28 R.A. Baggott, S.J. Rose, S.P.D. Mangles, Temperature equilibration due to charge state fluctuations in dense plasmas, Phys. Rev. Lett. **127**, 035002 (2021). https://doi.org/10.1103/PhysRevLett.127.035002

29 J. Simoni, J. Daligault, First-principles determination of electron-ion couplings in the warm dense matter regime, Phys. Rev. Lett. **122**, 205001 (2019). https://doi.org/10.1103/PhysRevLett.122.205001

30 J. Daligault, J. Simoni, Theory of the electron-ion temperature relaxation rate spanning the hot solid metals and plasma phases, Phys. Rev. E **100**, 043201 (2019). https://doi.org/10.1103/PhysRevE.100.043201

31 J. Simoni, J. Daligault, Calculation of electron-ion temperature equilibration rates and friction coefficients in plasmas and liquid metals using quantum molecular dynamics, Phys. Rev. E **101**, 013205 (2020). https://doi.org/10.1103/PhysRevE.101.013205

32 G. Faussurier, C. Blancard, Fast temperature relaxation model in dense plasmas, Phys. Plasmas **24**, 012705 (2017). https://doi.org/10.1063/1.4973225

33 C.E. Starrett, Coulomb log for conductivity of dense plasmas, Phys. Plasmas **25**, 092707 (2018). https://doi.org/10.1063/1.5053124

34 M. Oloumi, M. Habibi, H. Hosseinkhani, An analysis of the evaluations of Coulomb logarithm and electron–ion relaxation rates in deuterium plasmas across coupling regimes, Plasma Phys. Rep. **47**, 1021 (2021). https://doi.org/10.1134/S1063780X21100056

35 G.J.M. Hagelaar, Z. Donko, N. Dyatko, Modification of the Coulomb logarithm due to electron-neutral collisions, Phys. Rev. Lett. **123**, 025004 (2019). https://doi.org/10.1103/PhysRevLett.123.025004

36 L.B. Fletcher et al., Electron-ion temperature relaxation in warm dense hydrogen observed with picosecond resolved x-ray scattering, Front. Phys. **10**, 838524 (2022). https://doi.org/10.3389/fphy.2022.838524

37 A.S. Richardson, NRL Plasma Formulary (US Naval Research Laboratory); A.C. Hayes et al., Plasma stopping-power measurements reveal transition from non-degenerate to degenerate plasmas, Nat. Phys. **16**, 432-437 (2019). https://doi.org/10.1038/s41567-020-0790-3

38 J.R. Rygg, J.A. Frenje, C.K. Li, F.H. Séguin, R.D. Petrasso, D.D. Meyerhofer, C. Stoeckl, Electron-ion thermal equilibration after spherical shock collapse, Phys. Rev. E **80**, 026403 (2009). https://doi.org/10.1103/PhysRevE.80.026403

Мақала тарихы:
Түсті – 30.04.2025
Түзетілген түрде түсті – 06.07.2025
Қабылданды – 20.08.2025

Article history:
Received 30 April 2025
Received in revised form 6 July 2025
Accepted 20 August 2025

Авторлар туралы мәлімет:

1. **Мехди Кавехния** – Физика кафедрасы, Ғылым факультеті, Арак университеті, Арак, Иран; e-mail: nasrinhosseini_motlagh@iau.ir
2. **Хосейн Садеги** (автор-корреспондент) – Физика кафедрасы, Ғылым факультеті, Арак университеті, Арак, Иран; e-mail: H-sadeghi@araku.ac.ir
3. **Сейеде Насрин Хоссейнимолаг** – профессор, Физика кафедрасы, Шираз, Ислам Азад университеті, Шираз, Иран; e-mail: nasrinhosseini_motlagh@iau.ir

Information about authors:

1. **Mehdi Kavehnia** – Department of Physics, Faculty of Sciences, Arak University, Arak, Iran; e-mail: nasrinhosseini_motlagh@iau.ir
2. **Hossein Sadeghi** (corresponding author) – Department of Physics, Faculty of Sciences, Arak University, Arak, Iran; e-mail: H-sadeghi@araku.ac.ir
3. **Seyedeh Nasrin Hosseinimotlagh** – Prof., Department of Physics, Shi.,C., Islamic Azad University, Shiraz, Iran; e-mail: nasrinhosseini_motlagh@iau.ir